

The Scale-Adaptive Simulation Method for Unsteady Turbulent Flow Predictions. Part 1: Theory and Model Description

F. Menter¹ and Y. Egorov¹

¹ ANSYS Germany GmbH, Staudenfeldweg 12, 83624 Otterfing, Germany

Phone: +49(0)8024 9054 15

Fax: +49(0)8024 9054 17

E-mail: florian.menter@ansys.com

www.ansys.com

The article gives an overview of the Scale-Adaptive Simulation (SAS) method developed by the authors during the last years. The motivation for the formulation of the SAS method is given and a detailed explanation of the underlying ideas is presented. The derivation of the high-Reynolds number form of the equations as well as the calibration of the constants is provided. The concept of SAS is explained using several generic examples and testcases.

Keywords: turbulence model; scale-adaptive simulation; SAS; hybrid RANS-LES.

Abbreviations:

EARSM: explicit algebraic RSM;

DES: detached eddy simulation;

DIT: decaying isotropic turbulence;

HWN: high wave number (damping);

KSKL: K Square-root-K L (model)

LES: large eddy simulation;

MILES: monotonically integrated LES;

RANS: Reynolds-averaged Navier-Stokes (equations);

RSM: Reynolds stress model;

SAS: scale-adaptive simulation;

SKL: Square-root-K L (model);

SST: Shear-Stress Transport (model);

URANS: unsteady RANS;

WALE: wall-adapting local eddy viscosity (model).

Introduction

Since the introduction of two-equation models by Kolmogorov in 1942 (see Moffat [24], Wilcox [37]), they form the foundation of essentially all statistical turbulence models. Two-equation models reflect the basic idea that the minimum information required for modelling the effect of turbulence on the mean flow are two independent scales, obtained from two independent transport equations (e.g. Launder and Spalding, [11]). Two-equation models also form the core of higher order models like full Reynolds Stress models (RSM) (Rotta, [30], Launder et al., [12]) or Explicit Algebraic Reynolds Stress Models (EARSM) (Pope, [26], Rodi, [27], Gatski and Speziale, [9], Wallin and Johansson, [36]) or non-linear stress-strain models (Craft et al., [4]). Even one-equation models (Baldwin and Barth, [1], Menter, [14, 15], Spalart and Allmaras, [31]) using the eddy viscosity as a single variable, can be derived from two-equation models using equilibrium assumptions (Menter, [14, 15]).

From a more fundamental standpoint, all the currently used models suffer from lack of an underlying exact transport equation, which could serve as a guide for the model development on a term-by-term basis. The reason for this deficiency lies in the observation that the exact equation for ε (or ω) does not describe the large scales, but the dissipative scales. The goal of a two-equation model is however the modelling of the influence of the large scale turbulence on the mean flow. Due to the lack of an exact equation, the ε - and the ω -equations are modelled in analogy with the equation for the turbulent kinetic energy, k , using purely heuristic arguments. This has several disadvantages. The first is that important terms and physical effects can be missed in the derivation. The second is that additional effects like compressibility, buoyancy, etc. cannot be modelled on an exact basis.

A more consistent approach for formulating a scale equation has been developed by Rotta ([29, 30]). Instead of using purely heuristic and dimensional arguments, Rotta formulated an exact transport equation for kL , where L is an integral length scale of turbulence and k is the turbulent kinetic energy. Rotta's equation represents the large scales of turbulence and can therefore serve as a basis for

term-by-term modelling. The distinguishing factor of the model proposed by Rotta was the appearance of a length scale in the source terms of the kL -equation, involving a higher derivative of the velocity field. This resulted from the analysis of one of the terms in the exact equation. The availability of an inherent length scale is an attractive feature, because it allows a more subtle reaction of the model to resolved flow features. However, the third derivative proposed by Rotta turned out to be problematic and was never actually used in any of the kL -variants. There are several reasons for the omission of this term. The most important is that it is not intuitively clear, why the third derivative should be more relevant than the second derivative in determining the length scale. In addition, a third derivative is a tedious quantity to compute in a general-purpose CFD code and can easily result in numerical instabilities. With the omission of the higher derivative term, the kL -model lost its main distinguishing feature over the $k-\varepsilon$ and the $k-\omega$ models. Actually, without this term it proved inferior, as it could not be calibrated for the logarithmic profile without additional terms depending on wall distance. This deficiency has eventually led to the advent of the $k-\varepsilon$ model as the major industrial two-equation model. The following quote from Rodi [28] stresses that this was largely due to the kL -models inability of handling the log-layer: “In the late 60’s and early 70’s, some investigations have been carried out at Imperial College, London, with Rotta’s kL equation, but this requires an extra term near the wall to conform with the log law. Hence in the early 70’s there was soon a switch over to the $k-\varepsilon$ model ... By choosing the constants properly, the ($k-\varepsilon$) model can be made consistent with the log law.”

In recent years, steps of modernizing the kL -equation have been taken (Menter and Egorov, [17-20, 22]). It is argued that Rotta’s assumptions, leading to the term with the third derivative of the velocity field in his kL -equation, is not consistent with the nature of the underlying term in the exact equation. As a result, the second derivative appears in the model, satisfying the log-law without the need for additional terms. Furthermore, the model lends itself much easier to the introduction of robust low-Reynolds number (viscous sublayer model) extensions (Menter et al., [21]), than the $k-\varepsilon$ model. The new model has been re-formulated as a one- and a two-equation model using $\Phi = \sqrt{k}L$ as the new scaling variable in Menter et al. [21]. While the resulting KSKL ($k - \sqrt{k}L$) and SKL ($\sqrt{k}L$) models

offer interesting alternatives to existing steady RANS models, the more important aspect is their ability of resolving unsteady turbulent structures similar to the behaviour of Detached Eddy Simulation (DES) models (e.g. Spalart et al. [33], Spalart [32], Strelets [35]), but without an explicit influence of the grid spacing on the RANS part of the model.

The behaviour of the model in unsteady flow simulations will be the central subject of this article. Some of the underlying assumptions in the model derivation will be clarified and the concept of Unsteady RANS (URANS) will be discussed in light of the Scale-Adaptive Simulation (SAS) characteristics of the KSKL model. It will be shown that the classical URANS behaviour of current turbulence models is not a result of the averaging procedure applied to the equations, as widely thought in the community, but of the specific way RANS models were formulated in the past. This opens the way for using more advanced URANS concepts as a basis for unsteady simulations.

Rotta's k - kL Model

Basic Formulation

Almost all two-equation models use the equation for the turbulent kinetic energy, k , for determining one of the two independent large scales of turbulence. The principal unknown term in the k -equation is the turbulent dissipation rate, ε , which has to be obtained from another transport equation. While an exact equation for ε can be derived, it is not compatible with the need of describing the large scales of turbulence, as the dissipation takes place at the smallest scales of the turbulent spectrum. Similar arguments are true for ω , which is sometimes interpreted as the rate of dissipation per unit of turbulence kinetic energy (see Wilcox, [37]). In order of avoiding the difficulties associated with the exact ε -equation, the model equation for the dissipation rate is typically derived on dimensional arguments, avoiding a term-by-term modelling of the exact equation. Clearly, such a process bears the danger of missing essential physical effects, which might be contained in an exact equation system.

In order of providing a more solid foundation, Rotta [29] formulated an exact transport equation for the variable kL based on the definition of an integral length scale, L , and used it as a starting point of a term-by-term closure. This paragraph will give a short reminder of Rotta's derivation.

Assuming flows with a dominant shear strain in the y -direction (shear flows), the following length scale, L , can be defined (3/16 is an arbitrary scaling factor):

$$kL = \frac{3}{16} \int_{-\infty}^{\infty} R_{ii}(\bar{x}, r_y) dr_y \quad (1)$$

where k is the turbulent kinetic energy. In this equation, $R_{ii}(\bar{x}, r_y)$ is the sum of the diagonal the two-point correlation tensor measured at a location \bar{x} with two probes at distance r_y :

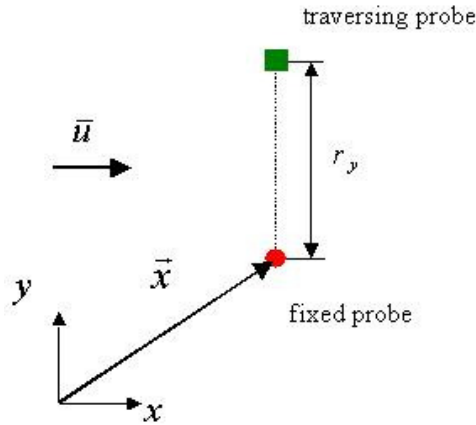


Figure 1: Two-point correlation measurement

In Figure 1, two probes are located at a distance r_y . They both measure the three fluctuating velocity components u_i . The correlation function R_{ii} is then defined as:

$$R_{ii} = \overline{u_i(\bar{x})u_i(\bar{x} + r_y)} \quad (2)$$

using the summation convention. The overbar represents a time (or ensemble) average. It is intuitively clear that the correlation function has a maximum at $r_y=0$ and decays to zero for large r_y , as sketched in Figure 2:

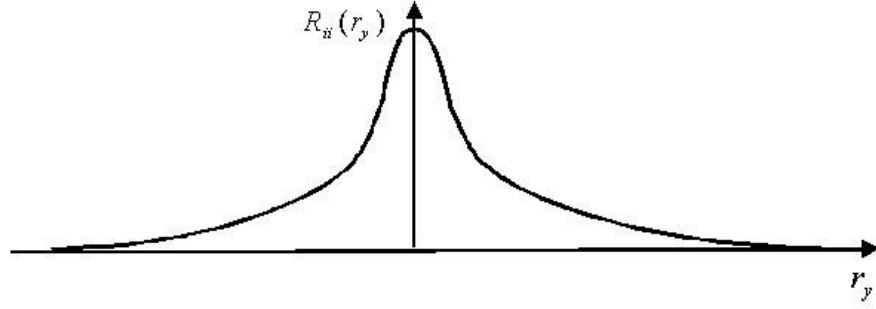


Figure 2: Two-point correlation

From Equation 1 it can be seen that the integral length scale, L , is proportional to the surface area under the correlation curve shown in Figure 2 divided by the turbulent kinetic energy, k . The two-point correlation allows therefore an exact definition of an integral length scale, L . Based on this definition, Rotta derived a transport equation for the quantity $\Psi = kL$ for shear flows. Including a time derivative (assuming ensemble averaging), the equation reads:

$$\begin{aligned}
 & \underbrace{\frac{\partial \Psi}{\partial t} + U_j \frac{\partial \Psi}{\partial x_j} + \frac{3}{16} \int_{-\infty}^{\infty} \left[\frac{\partial U(\bar{x} + r_y)}{\partial x} - \frac{\partial U(\bar{x})}{\partial x} \right] R_{ii} dr_y}_{\text{Convection}} = \\
 & \underbrace{-\frac{3}{16} \frac{\partial U(\bar{x})}{\partial y} \int_{-\infty}^{\infty} R_{21} dr_y - \frac{3}{16} \int_{-\infty}^{\infty} \frac{\partial U(\bar{x} + r_y)}{\partial y} R_{12} dr_y}_{\text{Production}} \\
 & \underbrace{+ \frac{3}{16} \int_{-\infty}^{\infty} \frac{\partial}{\partial r_k} (R_{(ik)i} - R_{i(ik)}) dr_y + \nu \frac{3}{8} \int_{-\infty}^{\infty} \frac{\partial^2 R_{ii}}{\partial r_k \partial r_k} dr_y}_{\text{Dissipation}} \\
 & \underbrace{- \frac{\partial}{\partial y} \left\{ \frac{3}{16} \int_{-\infty}^{\infty} \left[R_{(i2)i} + \frac{1}{\rho} (\overline{p'v'} + \overline{v'p'}) \right] dr_y - \nu \frac{\partial \Psi}{\partial y} \right\}}_{\text{Diffusion}}
 \end{aligned} \tag{3}$$

The first index below the integrals refers to the fixed probe location (grouping as indicated by parenthesis for three indices). The mean shear direction in this equation is aligned with the y -coordinate. The terms in the equation can be interpreted as convection, production, destruction and diffusion in the grouping as they appear above. U refers to the (time or ensemble) averaged velocity in x -direction.

Using this equation as a starting point, Rotta models the unknown correlations on a term-by-term basis. The first integral term on the left hand side can be neglected as it involves derivatives in x-direction, which are small compared to y-derivatives in shear layers. Therefore, this term is small compared to the integrals on the right hand side.

The most interesting term in Equation 3 is the second term on the right hand side:

$$-\frac{3}{16} \int_{-\infty}^{\infty} \frac{\partial U(\bar{x} + r_y)}{\partial y} R_{12} dr_y \quad (4)$$

containing the mean velocity gradient at the location of the second probe. In order of modelling this term, Rotta expands the velocity gradient into a Taylor series:

$$\frac{\partial U(\bar{x} + r_y)}{\partial y} = \frac{\partial U(\bar{x})}{\partial y} + \frac{\partial^2 U(\bar{x})}{\partial y^2} r_y + \frac{1}{2} \frac{\partial^3 U(\bar{x})}{\partial y^3} r_y^2 + \dots \quad (5)$$

which allows taking the derivatives outside the integral:

$$\begin{aligned} \int_{-\infty}^{\infty} \frac{\partial U(\bar{x} + r_y)}{\partial y} R_{12} dr_y &\rightarrow \\ \frac{\partial U(\bar{x})}{\partial y} \int_{-\infty}^{\infty} R_{12} dr_y + \frac{\partial^2 U(\bar{x})}{\partial y^2} \int_{-\infty}^{\infty} R_{12} r_y dr_y + \frac{1}{2} \frac{\partial^3 U(\bar{x})}{\partial y^3} \int_{-\infty}^{\infty} R_{12} r_y^2 dr_y + \dots \end{aligned} \quad (6)$$

The first term on the right hand side of this equation can be added to the existing production term in Equation 3. For the remaining terms, Rotta makes the assumption that the term with the second derivative of the mean velocity is negligible, leaving the term with the third derivative as the main additional contribution to the integral (higher order terms neglected). Furthermore, Rotta introduces the following definitions:

$$L_{12,1} = \frac{3}{16u_1' u_2'} \int_{-\infty}^{\infty} (R_{12} + R_{21}) dr_y \quad (7)$$

$$L_{12,n} = \left[\frac{3}{16(n-1)! u_1' u_2'} \int_{-\infty}^{\infty} R_{12} r_y^{n-1} dr_y \right]^{1/n}, \quad (n > 1)$$

and models them as:

$$L_{12,1} = \tilde{\zeta}_1 L, \quad L_{12,3} = \tilde{\zeta}_2 L^3 \quad (8)$$

The underlying assumption being that all lengths-scales based on the integrals in Equation 7 are proportional to one another.

The main destruction term is modelled based on dimensional arguments as:

$$-\frac{3}{16} \int_{-\infty}^{\infty} \frac{\partial}{\partial r_k} (R_{(ik)i} - R_{i(ik)}) dr_y = \tilde{\zeta}_3 \cdot k^{3/2} \quad (9)$$

Using a slightly simplified diffusion model (in Rotta's [30] notation it is assumed that $\alpha_L=1.0$), the final two-equation model can be written in the following boundary-layer form (y is a coordinate across a mixing layer):

$$\begin{aligned} \frac{\partial k}{\partial t} + U_j \frac{\partial k}{\partial x_j} &= P_k - c_\mu^{3/4} \frac{k^{3/2}}{L} + \frac{\partial}{\partial y} \left(\frac{v_t}{\sigma_k} \frac{\partial k}{\partial y} \right) \\ \frac{\partial \Psi}{\partial t} + U_j \frac{\partial \Psi}{\partial x_j} &= -\overline{u'v'} \left(\hat{\zeta}_1 L \frac{\partial U}{\partial y} + \hat{\zeta}_2 L^3 \frac{\partial^3 U}{\partial y^3} \right) - \hat{\zeta}_3 \cdot k^{3/2} + \frac{\partial}{\partial y} \left[\frac{v_t}{\sigma_\Psi} \frac{\partial \Psi}{\partial y} \right] \\ \Psi &= kL; \quad v_t = c_\mu^{1/4} \frac{\Psi}{\sqrt{k}} \end{aligned} \quad (10)$$

A factor of $c_\mu^{1/4}$ in the definition of the eddy viscosity corresponds to the selected definition of the length scale L , which returns $L=\kappa y$ in the logarithmic part of a near-wall boundary layer.

The constants for the Rotta [30] model are not fully specified but can be estimated as follows: $\hat{\zeta}_1 \approx 1.2$ based on correlation measurements from Rose (see Rotta, [30]) in a homogenous shear flow. Rotta further estimates that $\hat{\zeta}_3 \approx 0.11-0.13$ which covers the range of plausible Loitsianskii coefficients σ -2-4 for decaying isotropic turbulence. Assuming further a diffusion coefficient of $\sigma_\Psi \approx 1.0$ the value of $\hat{\zeta}_2$ can be calculated from the logarithmic layer requirements:

$$\hat{\zeta}_2 = -\frac{1}{2\kappa^2} \left(\hat{\zeta}_1 - \hat{\zeta}_3 \frac{1}{c_\mu^{3/4}} + \frac{1}{\sigma_\Psi} \kappa^2 \frac{1}{c_\mu^{1/2}} \right) \quad (11)$$

($\kappa=0.41$) giving values in the range of $\hat{\zeta}_2 \approx (-2.88) - (-3.24)$.

It is interesting to compare these values with those obtained from transforming the standard k - ε model coefficients into the k - kL model ($c_{\varepsilon 1} = 1.44$; $c_{\varepsilon 2} = 1.92$). The relation is:

$$\hat{\zeta}_1 = \frac{5}{2} - c_{\varepsilon 1}; \quad \hat{\zeta}_3 = c_{\mu}^{3/4} \left(\frac{5}{2} - c_{\varepsilon 2} \right) \quad (12)$$

Table 1: Model constants for k-kL model resulting from Rotta's and from the k- ε model

	$\hat{\zeta}_1$	$\hat{\zeta}_2$	$\hat{\zeta}_3$
Rotta	1.20	(-3.24) - (-2.88)	0.11-0.13
From k- ε	1.06		0.095

Obviously the k - ε model does not have a term corresponding to $\hat{\zeta}_2$ - the logarithmic layer can still be satisfied through the inclusion of the ε -diffusion term. It is also interesting that a negative value is required for $\hat{\zeta}_2$ in the Rotta's model, although the original integral is positive in a logarithmic layer.

Discussion of Rotta's Model

The principle difference of the kL -equation to other scale equations is the appearance of the third derivative of the velocity field. All other terms are equivalent to corresponding terms in the ω - or the ε -equation. This additional term is a result of the integral given by Equation 4 and the Taylor series expansion given in Equations 5-6. The main assumption made by Rotta is:

$$\frac{\partial^2 U(\bar{x})}{\partial y^2} \int_{-\infty}^{\infty} R_{12} r_y dr_y \approx 0 \quad (13)$$

leaving the third-derivative term as the leading order contribution. This estimate is based on the observation that in homogenous turbulence the function R_{12} is symmetric with respect to r_y . The product of $R_{12} r_y$ is therefore asymmetric and the integral becomes zero as the contributions from $-r_y$ balance the contributions from $+r_y$. This eliminates the second derivative term from the expansion and leaves the third derivative term as the leading scale-determining quantity.

There are several reasons why the third-derivative term is undesirable. The first is that it is physically non-intuitive. There is no physical reason, why the third derivative should have a strong influence on the definition of a turbulent length scale. The second reason why the third derivative is problematic is that it produces the incorrect sign in a logarithmic layer. The considered term in Equation 3:

$$-\frac{3}{16} \frac{1}{2} \frac{\partial^3 U(\bar{x})}{\partial y^3} \int_{-\infty}^{\infty} R_{12} r_y^2 dr_y \rightarrow -\overline{u'v'} \cdot \hat{\zeta}_2 L^3 \frac{\partial^3 U}{\partial y^3} \quad (14)$$

is positive in a logarithmic layer (R_{12} being mainly negative and the third derivative being positive). It therefore acts as a source term, instead of a sink term. However, a sink term is required in order to define a proper length scale. Based on the derivation of the term, it is not easily physically justified introducing a negative coefficient $\hat{\zeta}_2$. The final reason why the third derivative term should be avoided is that it is difficult to compute in a general purpose CFD code and that it is most likely erratic in a three-dimensional flow field.

However, without any higher derivative term, the model has no advantage compared to the scale equations derived solely on dimensional arguments. As mentioned above, it actually has a disadvantage as it does not allow satisfying the logarithmic layer.

The central question is therefore, whether the assumption:

$$-\frac{\partial^2 U(\bar{x})}{\partial y^2} \int_{-\infty}^{\infty} R_{12} r_y dr_y = 0 \quad (15)$$

is justified.

On closer inspection, the argument that the integral should be evaluated to zero is inconsistent. While it is true that the function R_{12} is symmetric in homogenous turbulence, the entire term would be zero under those conditions, as homogenous turbulence can only exist in a zero or constant shear environment (i.e.

$\partial^2 U / \partial y^2 = 0$). In other words, the term is an inhomogeneous term by its very nature. Menter and Egorov [17] argue therefore that the second derivative term should be kept as the leading order term in the equations, instead of the third

derivative. Interestingly, this term also provides the correct sign in a logarithmic layer.

Rotta's assumption concerning the second term in the Taylor series expansion had a strong and long-lasting effect on the history of turbulence modelling. Due to the problems with the third derivative, the community turned to the ε -equation instead (Rodi [28]), losing the ability of modelling length scale effects based on an exact transport equation. In addition, the ε -equation has proven notoriously difficult to be integrated through the viscous sublayer, a problem not observed in the kL model. This deficiency alone has resulted in large difficulties in the formulation of engineering turbulence models for decades. Even more interestingly, the kL model, using the second derivative exhibits an entirely different behaviour for unsteady flow simulations (termed SAS below), which is beneficial to many engineering flows, as will be shown below. When choosing the second velocity derivative instead of the third, this behaviour could have benefited Unsteady RANS (URANS) model simulations for several decades, offering an attractive alternative to Large Eddy Simulation (LES). One can argue that this behaviour for unsteady flows builds a natural bridge between RANS and LES and could have avoided the unnatural split of the turbulence community into an "engineering" RANS community and a "scientific" LES community, which has not been beneficial for either one of these two groups. Finally, the availability of SAS at an earlier stage would naturally have had a strong impact on hybrid RANS/LES model formulations. As will be shown below, the new SAS models can cover a significant portion of flows for which DES models have initially been developed.

The KSKL Model

Model Formulation

In the previous section, the argument has been made that the function R_{12} is not symmetric in inhomogeneous turbulence – thereby resulting in a non-zero value for the integral given in Equation 15. The heuristic correctness of this argument can best be explained for the flow in the logarithmic region of the law-of-the-wall.

In this thought experiment, shown in Figure 3, Probe 1 is fixed and Probe 2 is shifted by r_y . As the size of the large turbulent eddies increases linearly with distance from the wall like $L = \kappa y$, it is clear that configuration I in Figure 3 will result in a smaller correlation than configuration II. Therefore, the correlation measured in configuration III is asymmetric with respect to $\pm r_y$. As a result, the integral of Equation 15 is non-zero.

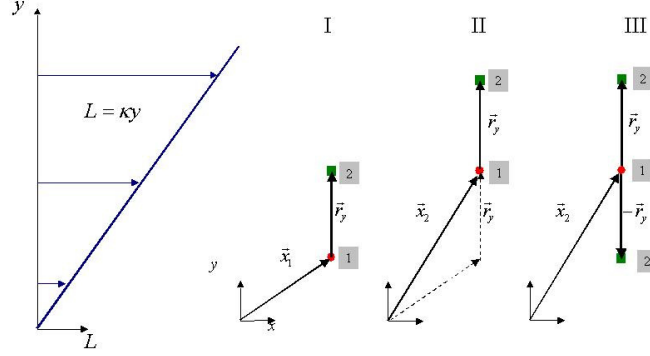


Figure 3: Hypothetical experiment in logarithmic layer

In early papers on the new model (e.g. Menter and Egorov, [17]), a linear dependency of the term in Equation 15 on the second velocity derivative was proposed, whereas in the latest version a quadratic formulation is used (Menter et

al., [21]). It is clear that the integral itself $\int_{-\infty}^{\infty} R_{12} r_y dr_y$ should be zero for

homogenous turbulence due to the symmetry of the two-point correlations in homogenous flows (Rotta's argument). In other words, this term should be proportional to a quantity which is zero under homogenous conditions. Here we assume the ratio of the turbulent length scale to the von Karman length scale

$L_{vK} = \kappa \left| \frac{\partial U / \partial y}{\partial^2 U / \partial y^2} \right|$ as the non-dimensional indicator for "non-homogeneity" (note

that L/L_{vK} goes to zero for homogeneous shear):

$$\int_{-\infty}^{\infty} R_{12} r_y dr_y = \text{const} \cdot \overline{u'v'} L^2 \frac{L}{L_{vK}} \quad (16)$$

Based on this, the following modelled form of the integral term is therefore proposed (κ absorbed in const.):

$$\begin{aligned}
-\frac{3}{16} \frac{\partial^2 U(\bar{x})}{\partial y^2} \int_{-\infty}^{\infty} R_{12} r_y dr_y &\rightarrow -const \cdot \overline{u'v'} \cdot L^2 \frac{\partial^2 U}{\partial y^2} \frac{L}{L_{vK}} = \\
&+ const \cdot \overline{u'v'} \cdot L^2 \left(\frac{\partial U / \partial y}{L_{vK}} \right) \frac{L}{L_{vK}} = \\
&- const \cdot \frac{\Psi}{k} P_k \left(\frac{L}{L_{vK}} \right)^2
\end{aligned} \tag{17}$$

The transformation in Equation 17 involves the recognition that the second derivative of U is negative in logarithmic layers. Taking its absolute value therefore results in a change of sign of the entire term.

All other terms are modelled like in Rotta's model:

$$\frac{\partial \Psi}{\partial t} + U_j \frac{\partial \Psi}{\partial x_j} = \frac{\Psi}{k} P_k \left(\tilde{\zeta}_1 - \tilde{\zeta}_2 \left(\frac{L}{L_{vK}} \right)^2 \right) - \tilde{\zeta}_3 \cdot k^{3/2} + \frac{\partial}{\partial y} \left[\frac{v_t}{\sigma_\Psi} \frac{\partial \Psi}{\partial y} \right] \tag{18}$$

In order to distinguish this new Ψ model Equation (18) from the original Rotta Equation (10) the model parameters are written here with a tilde overbar $\tilde{\zeta}_i$ rather than with a caret overbar $\hat{\zeta}_i$.

While this equation represents a proper scale equation, which could serve as a basis for calibration, it was decided [21] for practical reasons to introduce a further step in the derivation and transform the equation to a new variable $\Phi = \sqrt{k}L$. This variable has the advantage of being directly proportional to the eddy viscosity and therefore allows formulating a one-equation model in addition to the proposed two-equation model (see Menter et al., [21]). A simple transformation of variables leads to the final two-equation model formulation, written in the full three-dimensional form (omitting overbars from now on):

$$\frac{\partial(\rho k)}{\partial t} + \frac{\partial(\rho U_j k)}{\partial x_j} = P_k - c_\mu^{3/4} \cdot \rho \frac{k^2}{\Phi} + \frac{\partial}{\partial x_j} \left(\frac{\mu_t}{\sigma_k} \frac{\partial k}{\partial x_j} \right)$$

$$\frac{\partial(\rho \Phi)}{\partial t} + \frac{\partial(\rho U_j \Phi)}{\partial x_j} = \frac{\Phi}{k} P_k \left(\zeta_1 - \zeta_2 \left(\frac{L}{L_{vK}} \right)^2 \right) - \zeta_3 \cdot \rho k + \frac{\partial}{\partial x_j} \left(\frac{\mu_t}{\sigma_\Phi} \frac{\partial \Phi}{\partial x_j} \right) \quad (19)$$

$$\mu_t = c_\mu^{1/4} \rho \Phi; \quad L_{vK} = \kappa \frac{U'}{U''}; \quad \text{with } U'' = \sqrt{\frac{\partial^2 U_i}{\partial x_k^2} \frac{\partial^2 U_i}{\partial x_j^2}}; \quad U' = \sqrt{2 \cdot S_{ij} S_{ij}}$$

In the transformation, cross-diffusion terms containing derivatives of k have been avoided. These terms result from the transformation of the diffusion term in Equation 18. Since this term is a modelled term, there is no reason why the diffusion model of Equation 18 should be more accurate than the one of Equation 19. It should also be noted that the omitted terms do not affect the calibration of the constants, as they are zero in the logarithmic layer. For completeness, the density was introduced into the equations.

The relationship between the constants of the new model and Rotta's model is (see Table 1):

$$\zeta_1 = \hat{\zeta}_1 - \frac{1}{2}; \quad \zeta_2 = \zeta_1 - c_\mu^{-3/4} \zeta_3 + c_\mu^{-1/2} \frac{\kappa^2}{\sigma_\Phi}; \quad \zeta_3 = \hat{\zeta}_3 - \frac{1}{2} c_\mu^{3/4}; \quad \sigma_\Phi = \sigma_\Psi \quad (20)$$

where ζ_2 comes from the logarithmic layer relationship.

Table 2: Model constants for k - Φ model (current version and transformation from Rotta)

	ζ_1	ζ_2	ζ_3	σ_k	σ_Φ
From k - Ψ	0.7		0.0278-0.0478	1	1
k - Φ [21]	0.8	1.47	0.0288	2/3	2/3

Parameter values, resulting from a direct transformation of the constants from the Rotta's model, are presented in the first row of Table 2 (note that ζ_2 cannot be obtained from the transformation, due to the difference between the 2nd and 3rd derivative). The second row of the constants are those proposed in Menter et al. [21] after some optimization for a range of boundary layer and free shear flows (ζ_2 results from the logarithmic law). It should be noted that the calibration of the constants is not considered final, but is also not critical for the purpose of the

present article concentrating on the unsteady behaviour of the model. In Menter et al. [21] there are more details concerning the integration of the model through the viscous sublayer and the relationship between a one- and two-equation formulation. The terminology “KSKL model” results from $k - \sqrt{k}L$ (**K**-Square-root **K L**).

The emphasis of the current article is on the unsteady characteristics of the KSKL model. However, in order to demonstrate that the model is a suitable RANS formulation, Figure 4 shows a comparison of velocity profiles for steady state computations around the NACA 4412 airfoil of Coles and Wadcock [2]. The figure shows a comparison of the KSKL (two-equation model), SKL (Square-root-**K L**) (one-equation model) as given in Menter et al. [21], the SST and the Spalart and Allmaras [31] model for the NACA 4412 airfoil of Coles and Wadcock [2] at 13.9° and $Re=1.5 \cdot 10^6$. It can be seen that the optimized version of the KSKL (and the related SKL) model are competitive against the more established one- and two-equation turbulence models.

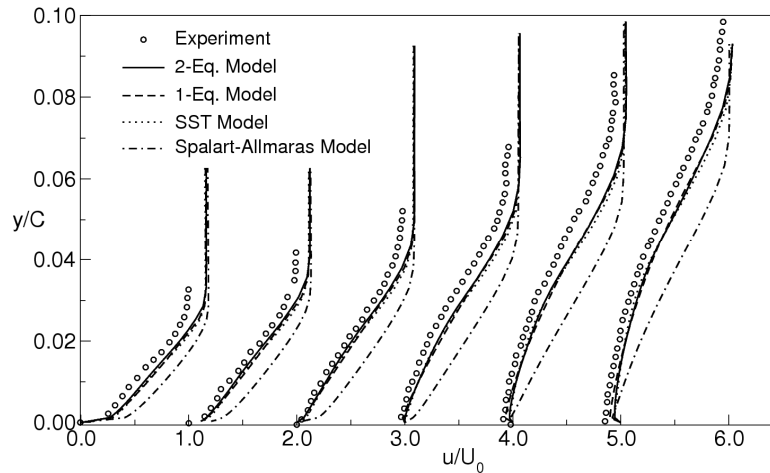


Figure 4: Velocity profiles at the upper surface around the trailing edge separation zone for NACA 4412 airfoil. (1-Eq. SKL, 2-Eq. KSKL model – both models are extensions of the basic version given here).

Physical Interpretation

The exact transport equation underlying the current model indicates that higher derivatives of the velocity field should appear in the scale equation. It is

interesting to go back to Rotta's interpretation of the influence of such terms. In his book [30] Rotta states (translated from German): "Neglecting the convective and diffusive terms and replacing $c \cdot k^{3/2}$ with the help of the equation for the turbulent kinetic energy, one obtains the following interesting simplification:

$$L^2 = 2\kappa^2 \frac{\partial U / \partial y}{\partial^3 U / \partial y^3} \quad (21)$$

This relation has a remarkable similarity to the formula:

$$L_{vK} = \kappa \left| \frac{\partial U / \partial y}{\partial^2 U / \partial y^2} \right| \quad (22)$$

which von Karman derived based on similarity arguments".

This statement indicates, that Rotta viewed it as one of the main characteristics of his model, that it provided a natural length scale through the source terms, which is missing in all other models. In other words, forming a source term equilibrium using k - ε or k - ω type models does not allow the determination of a length L (or related) scale. This can best be seen from the standard k - ω model:

$$\begin{aligned} \frac{\partial(\rho k)}{\partial t} + \frac{\partial(\rho U_j k)}{\partial x_j} &= \rho \frac{k}{\omega} (S^2 - c_\mu \omega^2) + \frac{\partial}{\partial x_j} \left(\frac{\mu_t}{\sigma_k} \frac{\partial k}{\partial x_j} \right) \\ \frac{\partial(\rho \omega)}{\partial t} + \frac{\partial(\rho U_j \omega)}{\partial x_j} &= \rho (c_{\omega 1} S^2 - c_{\omega 2} \omega^2) + \frac{\partial}{\partial x_j} \left(\frac{\mu_t}{\sigma_\omega} \frac{\partial \omega}{\partial x_j} \right) \end{aligned} \quad (23)$$

When considering the turbulence model source terms as a black box, the only variable entering from the outside is the shear strain rate $S \sim 1/T$. The source terms can therefore only help determining one turbulence scale – in this case the turbulent frequency $\omega \sim (1/T) \sim S$. The second scale is not defined from the source terms alone.

Despite the widespread usage of two-equation models their mechanism of determining the turbulent length scale is often not appreciated. It results from the inclusion of the diffusion terms into the estimate as follows (for a generic variable Θ):

$$\frac{\partial}{\partial y} \left(\frac{\nu_t}{\sigma} \frac{\partial \Theta}{\partial y} \right) \propto \nu_t \frac{\Theta}{\delta^2} \quad (24)$$

where δ is the thickness of the turbulent layer (shear layer thickness). Introducing this estimate into standard two-equation models gives:

$$L \sim \delta \quad (25)$$

In other words, the turbulent length scale, L , calculated by a standard two-equation model, will always approach the thickness of the turbulent layer. As stated by Rotta [30], models based on the kL equation behave differently – they allow the determination of both turbulent scales from the source terms of the models. In the case of the KSKL model, the estimate is $L \sim L_{vK}$.

What is the physical meaning of the additional source term, containing L_{vK} ? Obviously any spatial variation in the strain rate (meaning a non-zero second derivative) reduces the effectiveness of the production term in the Φ equation. Figure 5 and Figure 6 illustrate the physical plausibility of this model. Under constant shear (homogenous conditions, Figure 5) the turnover frequencies of two small eddies are the same independent of their location, as they are driven by the same constant strain rate, S . They can therefore merge into one larger vortex with the same turbulent frequency. This corresponds to the actual situation in constant shear flows – the turnover frequency of turbulence is proportional to the strain rate while the length scale grows to infinity.

Under non-homogenous conditions (strain rate not constant, Figure 6), the individual vortices have locally different turnover frequencies proportional to the local strain rate. From a certain size on, they can therefore not merge into a larger vortex, as one vortex cannot have two different frequencies. This results in a finite vortex size depending on the local strain rate and its spatial variation. The spatial variation is given to first order by the von Karman length scale. This is the physical rationale why the von Karman length scale should appear in the length scale equation of a RANS model formulation. Note that the application of a standard two-equation model to a frozen parabolic mean flow would result in an infinite length scale, as there is no finite layer thickness – this is intuitively incorrect.

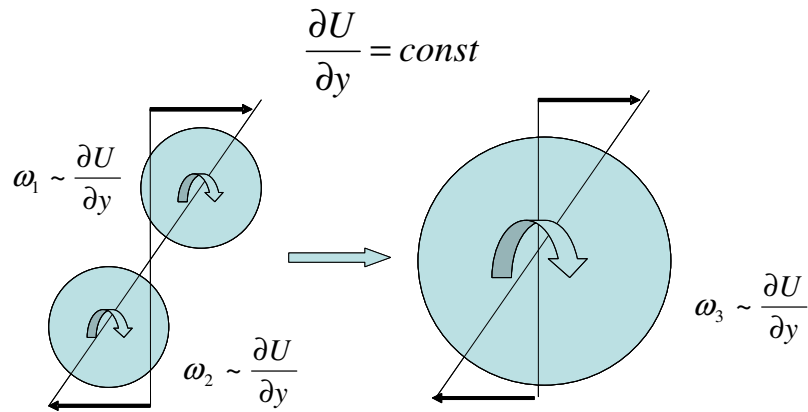


Figure 5: Turbulent eddies under homogenous (constant) strain. Two small eddies with equal turbulent frequency form one larger eddy.

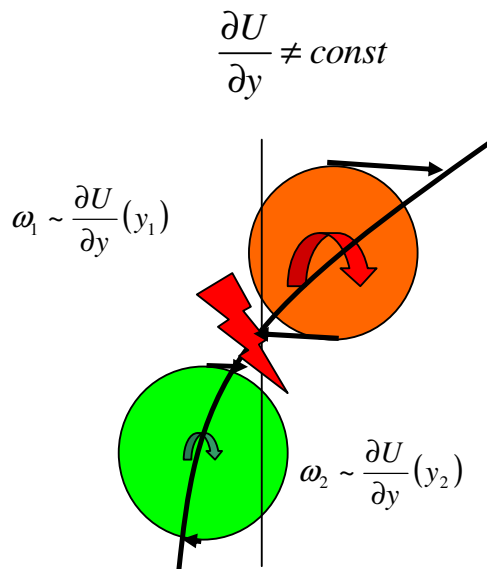


Figure 6: Turbulent eddies under non-homogenous strain. Individual eddies have different turnover frequencies and cannot merge into larger eddy.

It is important to note that under certain conditions, the entire production term in the Φ Equation (19) can and should become negative. Assume one could enforce a parabolic velocity profile (e.g. through external volume forces) and would start with turbulent vortices significantly larger than dictated by the von Karman length scale, L_{vK} , then the interaction between the large vortices and the mean velocity

gradient would lead to the destruction of the large turbulent eddies until they are compatible with the specified velocity field.

Another interesting situation arises in the following generic experiment.

Assuming again that a 1-D mean flow profile of the form $U(y)=U_0 \times \sin(\lambda y)$ could be established by external (e.g. magnetic) forces. This mean flow has a characteristic length $L_r \sim 1/\lambda$. Under such conditions, one would assume that the turbulence model would provide a modelled scale which is also $L \sim 1/\lambda$ as only scales smaller than $1/\lambda$ have to be modelled (it is physically intuitive that no larger turbulent structures can exist in such a mean flow). Nevertheless, standard two-equation models will return an infinite value for L , as no layer thickness is imposed in this flow. If a finite layer thickness is imposed (e.g. by specifying walls at $y_\delta = \pm \delta/2$) the models would return $L \sim \delta$ again in contradiction with the expectation $L \sim 1/\lambda$. The new family of models with L_{vK} actually recognizes the inherent scale of the mean flow and provides the expected result $L \sim 1/\lambda$, independent of the size of the layer thickness. This characteristic of the model is termed “Scale-Adaptive Simulation - SAS”, as the model can adjust to already existing (resolved) scales.

All arguments so far have been based on steady state (RANS) considerations. It should be emphasized that the KSKL model is derived entirely based on RANS arguments – and arguably in the most consistent way by starting from an exact transport equation. However, the above SAS behaviour of the model opens some fundamental questions, concerning unsteady flow simulations. The most interesting question is, whether the model allows the formation of a turbulent spectrum. This was tested by applying the model to the unsteady flow simulation around a cylinder in crossflow. Figure 7 shows a comparison of the solutions obtained with the SST and the KSKL model. It is clear that the KSKL model allows the formation of turbulent structures, not observed in the SST or other URANS models.

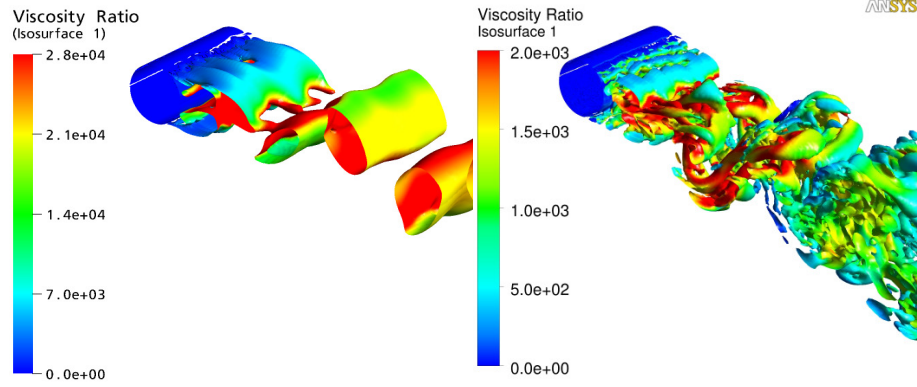


Figure 7: Circular cylinder in a cross flow at $Re=3.6 \cdot 10^6$, Left: SST-URANS, Right: KSKL model. Iso-surface of $Q=S^2-\Omega^2$, coloured according to the eddy viscosity ratio μ_t/μ (smaller by factor 14 in right figure)

How is this possible, considering that the model was derived based on averaged equations? The answer depends partly on the question: to which scale will the von Karman length scale adjust, given a resolved turbulent flow with a Kolmogorov spectrum is provided:

$$E(k) \sim k^{-5/3} \quad (26)$$

where k is the wave number. This implies for the velocity derivatives:

$$U'(k) \sim k^{1/6}; \quad U''(k) \sim k^{7/6} \quad (27)$$

meaning that both first and second velocity derivatives are dominated by the smallest scales! The von Karman length scale, L_{vK} , is therefore determined by the smallest scales in the spectrum. In other words, L_{vK} adjusts to the smallest scales resolved. This is a pre-requisite for allowing the formation of the turbulent spectrum.

A standard test for the unsteady characteristics of the model is Decaying Isotropic Turbulence (DIT). The interest is not in running DIT in RANS mode, meaning simply specifying values for k and Φ and following their decay as given by their corresponding transport equations. Instead the DIT case is run in “LES”-mode, meaning an initially resolved velocity field is specified and its decay is computed. In order to obtain initial conditions for k and Φ , the KSKL model equations are solved given the frozen resolved initial velocity field (it is again interesting to

point out that standard two-equation models would not provide converged solutions under such conditions, as the flow is computed with periodic boundary conditions, not providing a finite layer thickness). Using these initial conditions, the KSKL model is then run coupled with the flow equations. In addition, solutions with the LES-WALE model and the standard $k-\varepsilon$ model are also computed (for $k-\varepsilon$ the transformed initial conditions of the KSKL model are used). Simulations are computed on a 32^3 grid using a 2^{nd} order central scheme for the convective fluxes.

Figure 8 shows the turbulent spectrum for the Comte-Bellot experiment (Comte-Bellot and Corrsin, [3]) in comparison with the experimental data after $t=2$ non-dimensional times. The most interesting result is that the KSKL model allows the formation of a turbulent spectrum, but does not provide sufficient damping at the high-wave number limit to dissipate the energy at the smallest scales. This is in obvious contradiction to the expectations for URANS models and the new central aspect of the model. The $k-\varepsilon$ model behaves as expected and damps out the small scales quickly, while the WALE model returns its calibrated behaviour in agreement with the experimental spectrum. Considering the above arguments, the behaviour of the KSKL model is actually not all that surprising, as the von Karman scale adjusts to the smallest scales and thereby produces an eddy viscosity small enough to allow the formation of even smaller eddies until the grid limit is reached. At that point, no smaller eddies can form. However, consistently, the partial differential equations of the SAS model, having no information on the cut-off limit again provide an eddy viscosity small enough to allow further cascading to smaller scales. As this is not possible due to the resolution limit, the energy accumulates at the high wave number limit. The behaviour of insufficient damping can easily be augmented for practical flow simulations, as will be shown later. This behaviour, however, is of significant theoretical interest as it contradicts the common expectations concerning URANS models.

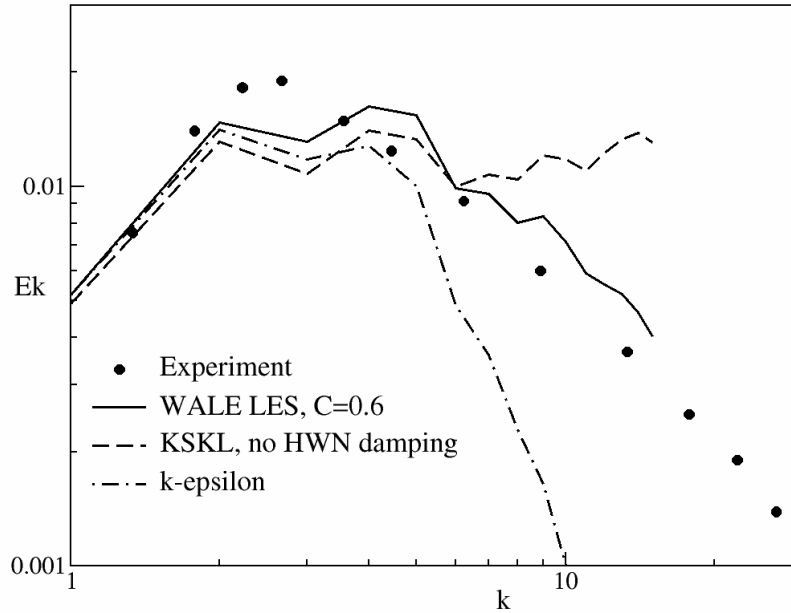


Figure 8: Turbulent Spectrum for DIT in comparison with exp. Data. LES – WALE model, KSKL – without High Wave Number (HWN) Damping at time $t=2$.

This is a good point for reconsidering the situation. First a new turbulence model based entirely on RANS arguments has been derived. It was found that this model can be calibrated to produce steady RANS solutions for numerous flows like the airfoil flow shown above, or other flows computed by Menter et al. [21]. However, under certain conditions, the model violates the expectations concerning RANS models and allows the formation of a turbulent spectrum down to the grid limit. As RANS is based on averaging out random fluctuations, this points to a conceptual problem in the definition of RANS (and more so URANS) models. While classical RANS models like $k-\epsilon$ do not show this discrepancy, they do however instead produce a disturbing and unphysical behaviour for the generic flows discussed above. Especially for the generic 1-D mean flow $U(y)=U_0 \times \sin(\lambda y)$ it is unphysical that standard models return $L \rightarrow \infty$. In other words, both types of models produce results which are intuitively in contradiction with expectations. The choice is between models which either do not recognize resolved scales at all and thereby allow length scales larger than the driving flow scale, or models which do adjust to resolved structures and as a result allow the formation of a turbulent spectrum as long as the numerical method and the grid and time step allows it. Which behaviour is “correct” cannot be determined, as

both types of models are derived on suitable RANS arguments. One could even argue that the KSKL model has a stronger theoretical RANS foundation, as it uses an exact transport equation as a starting point.

Leaving aside the theoretical considerations and turning to more practical aspects, the new model offers an interesting passage into scale-resolving simulations. Given that a sufficiently strong instability or an initially resolved flow is present, the model allows the formation of a turbulent spectrum, similar to an LES model. At the same time, stable flow regions will still be covered in RANS mode. This indicates a behaviour similar to the Detached Eddy Simulation (DES) concept proposed by Spalart et al. ([32], [33]), but on an entirely different basis and using different modelling mechanisms. Some practical results for unsteady simulations using the KSKL model will be shown below and in Egorov et al. [7].

High Wave Number (HWN) Damping

The tests for the DIT case have shown that the KSKL model (and other SAS models) does not provide sufficient damping of the smallest scales at the grid limit. This is not a difficult practical problem, as classical LES technologies can be applied for achieving the required dissipation of energy. The simplest and most pragmatic way of achieving this goal has turned out to be the enforcement of a lower limit on the eddy viscosity coming from the SAS model. The lower limit should however not impact steady state RANS solutions. This could be achieved by a dynamic LES model, which returns near-zero eddy viscosity for steady state RANS flows. A simpler and also satisfactory formulation results from using the WALE LES model (Nicoud and Ducros, [25]) for this purpose:

$$\nu_t = c_\mu^{1/4} \Phi \quad \rightarrow \quad \nu_t = \max\left(c_\mu^{1/4} \Phi, \nu_t^{WALE}\right) \quad (28)$$

(It might be worthwhile to point out that DES models can be formulated by replacing the *max* function in Equation 28 by a *min* function and using suitably defined RANS and LES models). Figure 9 shows the turbulent spectrum for the DIT case computed without and with the limiter.

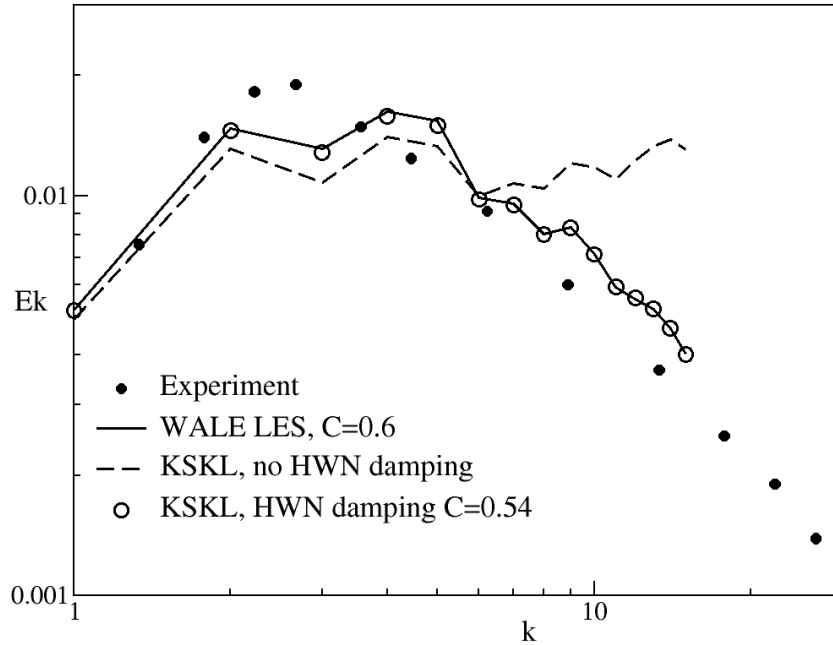


Figure 9: Turbulent spectrum for DIT in comparison with experimental data. The result by the KSKL model with HWN damping (circles) coincides with the WALE LES result (solid line). C is a constant in WALE model.

There is another practical advantage to the specification of a classical LES model as a lower limit. Experience over the last years has shown that SAS-resolved solutions are often questioned in terms of their LES characteristics. However, if the SAS model reaches an established LES model limit in unstable flow regimes, it is clear that a “proper” LES formulation is achieved. For the DIT case, the ratio of ν_t^{WALE} / ν_t is equal to one. As this limit is reached, any arguments that SAS does not produce a correct LES limit are easily invalidated.

Transformation to other primary variables

The KSKL model can be transformed to other variables, which can help introducing the unsteady characteristics of this model into existing two-equation models. The high Reynolds number equations for k - ϵ and k - ω are (assuming $\sigma_k = \sigma_\phi$):

$$\begin{aligned} \frac{\partial \rho \varepsilon}{\partial t} + \frac{\partial \rho U_j \varepsilon}{\partial x_j} = & \frac{\varepsilon}{k} P_k \left(2 - \zeta_1 + \zeta_2 \left(\frac{L}{L_{vK}} \right)^2 \right) - \rho \frac{\varepsilon^2}{k} \left(2 - \frac{\zeta_3}{c_\mu^{3/4}} \right) \\ & + \frac{\partial}{\partial x_j} \left(\frac{\mu_t}{\sigma_\Phi} \frac{\partial \varepsilon}{\partial x_j} \right) - \frac{2c_\mu \rho}{\sigma_\Phi} \left(\frac{k^4}{\varepsilon^2} \frac{\partial}{\partial x_j} \left(\frac{\varepsilon}{k} \right) \frac{\partial}{\partial x_j} \left(\frac{\varepsilon}{k} \right) \right) \end{aligned} \quad (29)$$

$$\begin{aligned} \frac{\partial \rho \omega}{\partial t} + \frac{\partial \rho U_j \omega}{\partial x_j} = & \frac{\omega}{k} P_k \left(1 - \zeta_1 + \zeta_2 \left(\frac{L}{L_{vK}} \right)^2 \right) - \rho \omega^2 (c_\mu - c_\mu^{1/4} \zeta_3) \\ & + \frac{\partial}{\partial x_j} \left(\frac{\mu_t}{\sigma_\Phi} \frac{\partial \omega}{\partial x_j} \right) + \frac{2\rho}{\sigma_\Phi} \left(\frac{1}{\omega} \frac{\partial k}{\partial x_j} \frac{\partial \omega}{\partial x_j} - \frac{k}{\omega^2} \frac{\partial \omega}{\partial x_j} \frac{\partial \omega}{\partial x_j} \right) \end{aligned} \quad (30)$$

To complete the model derivation, the additional terms have also been introduced into the widely used SST model (Menter, [13]). For details on how the term with the von Karman length scale is introduced into the SST model see Egorov and Menter [6]. The formulation results in an additional term in the ω -equation of that model (added to the right hand side):

$$Q_{SAS} = \max \left[\rho \zeta_2 S^2 \left(\frac{L}{L_{vK}} \right)^2 - C_{SAS} \frac{2\rho k}{\sigma_\Phi} \max \left(\frac{1}{k^2} \frac{\partial k}{\partial x_j} \frac{\partial k}{\partial x_j}, \frac{1}{\omega^2} \frac{\partial \omega}{\partial x_j} \frac{\partial \omega}{\partial x_j} \right), 0 \right] \quad (31)$$

with $C_{SAS}=2$. The *max* function and the k -derivative term have been introduced to avoid any change to the SST models RANS performance for boundary layer flows. In unsteady situations, the term including the von Karman length scale is dominating the other terms resulting in the full activation of the SAS functionality. The resulting model is termed SST-SAS model.

Numerical Treatment

No proper LES behaviour can be achieved with an overly dissipative numerical treatment of the convective terms. In industrial LES, the usage of 2nd order central discretisation (CD) schemes is an established technology. However, pure CD schemes are not suitable for RANS portions in the flow. This situation is also present in hybrid models like DES, where typically a switching function is used for applying CD in LES regions, and higher order upwind schemes in the RANS parts. The method proposed by Strelets [35], is also applied to the current implementation in ANSYS-CFX. An alternative is the usage of a Bounded CD

(BCD) scheme as described in Kim [10]. This formulation is currently used in ANSYS-Fluent.

Finally, it should be noted that the discretisation of the second derivative of the velocity field required for the von Karman length scale, should be computed on a compact stencil, involving only three nodes in a 1-D flow.

Scale-Adaptive Simulation

In the previous chapters, the expression “Scale-Adaptive Simulation - SAS” has been used several times without a detailed explanation of its meaning. The terminology is essentially based on a URANS model’s ability of adjusting to resolved structures in a flowfield through its source terms (source term equilibrium). In contrast, classical RANS models adjust the length scale to the shear layer thickness, independent of any resolved scales, thereby suppressing the formation of turbulent structures. It is widely believed that this behaviour is a necessary consequence of the Reynolds averaging and therefore an inevitable feature of all RANS models. If nothing else, the derivation of the KSKL model and its demonstrated behaviour for unsteady flow predictions show that this belief is incorrect.

This seems confusing – “how can a model which is derived on Reynolds averaging resolve unsteady structures?” The answer is simply: “the equations have no memory of their derivation” (Menter et al., [16]). In other words, the fact that the equations have been Reynolds averaged is only known by the human observer, the information handed to the momentum equations is only the eddy viscosity (or the Reynolds stresses). If the eddy viscosity is small enough, the model allows the formation of a turbulent spectrum, provided the flow is sufficiently unstable. It is important to note that the momentum equations for LES and RANS are identical even though their derivation is entirely different (assuming an eddy viscosity model is used in both concepts). In other words, it is not the averaging concept which defines the equations, but the details of the turbulence model formulation.

The KSKL model and other variants of SAS formulations provide an eddy viscosity small enough to allow a break-up of large scales into smaller ones under unstable flow situations. Unfortunately, there is no theoretical criterion with respect to when a flow is sufficiently unstable to produce such a mode. It is very likely that this will depend on the specific formulation of the SAS model (e.g. a combination of an SAS scale equation with a Reynolds stress model might be less stable than a simple eddy viscosity formulation). Nevertheless, there are classes of flows for which a resolution down to the grid limit is typically achieved. Examples are massively separated flows on the leeward side of bluff bodies or strongly swirling flows etc. The industrial applications of the model already cover a significant range of flows (see Egorov et al [7]):

In order of avoiding multiple definitions and naming conventions, as observed in DES, the following definition is given for SAS models, (Menter and Egorov, [20]).

“SAS modelling is based on the use of a second mechanical scale in the source/sink terms of the underlying *high-Reynolds number* turbulence model. In addition to the standard input from the momentum equations in the form of first velocity derivatives (strain rate tensor, vorticity tensor, ...) SAS models rely on a second scale, typically in the form of higher velocity derivatives (here a second derivative). This is done in a way which allows the model to adjust its length scale to resolved structures in the flow”

SAS models satisfy the following requirements:

- Provide proper RANS performance in stable flow regions (boundary layer, channel flow, etc.)
- Allow the break-up of large turbulent structures into a turbulent spectrum for unstable flow regimes (cylinder in crossflow, airfoil at high angles of attack, flow in cavities, ...)
- Provisions for providing proper damping of resolved turbulence at the high wave number end of the spectrum (resolution limit of the grid) (DIT).

- Contrary to DES and related methods, the first two points are achieved without an explicit grid or time step dependency in the RANS model. Only the third requirement has to be based on information on the grid spacing, other information concerning the resolution limit (dynamic LES model, etc.), or the numerical method (MILES damping etc.).

Figure 10 shows a visual example of scale-adaptivity for the periodic hill flow (Fröhlich et al., [8]). The three pictures show the Q-criterion for three simulations of this flow. The left picture was computed with a time step of $\Delta t = 0.045 U_B/h$ (U_B – bulk velocity, h - height of hill) which corresponds to an LES time resolution. The middle and the right pictures were obtained using a factor 2 and 4 larger Δt on the same numerical mesh ($2.5 \cdot 10^6$ nodes). The colour of the figures depicts the ratio of eddy viscosity to molecular viscosity. The larger time steps do not allow the same spatial resolution as the small ones, resulting in significantly larger turbulent structures. The important aspect is that the eddy viscosity adjusts accordingly and increases from left to right. It thereby compensates for the non-resolved portion of the spectrum. Further increasing the time step will result in a steady RANS solution. Figure 11 shows the time-averaged velocity profiles for the different simulations compared to a steady-state RANS solution using the SST model. For SAS, only the smallest and largest Δt results are shown for clarity. Even for the largest Δt , there is a clear improvement compared to RANS.

It is interesting to consider the behaviour of a classical Smagorinsky LES model ($\nu_t = (c\Delta)^2 S$) for this situation. As the grid is the same in all three simulations, and as the strain rate is lower for large scales than for small scales, one would obtain actually the opposite behaviour. The Smagorinsky model would predict a lower eddy viscosity for the larger structures and is therefore not scale-adaptive. This behaviour would also carry over to DES methods, as they scale like the Smagorinsky model once the DES limiter is activated.

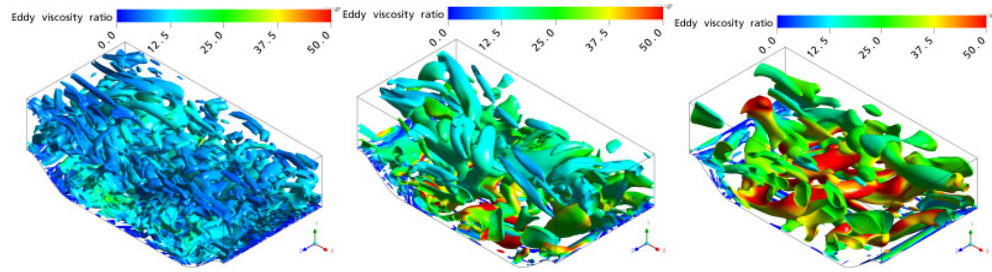


Figure 10: Turbulent structures for periodic hill flow. Iso-surface for $Q=S^2-\Omega^2$. Colour gives the eddy viscosity ratio μ_t/μ (increases from left to right by factor ~ 10). Left: $\Delta t=0.045U_B/h$, middle: $\Delta t=0.09U_B/h$, right: $\Delta t=0.18U_B/h$

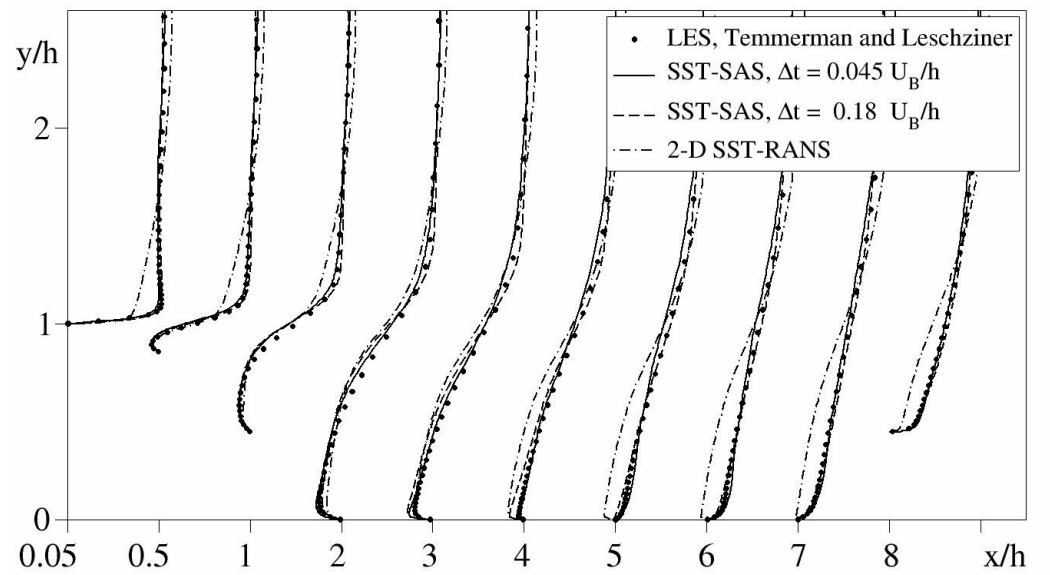


Figure 11: Mean velocity profiles for periodic hill comparing SAS for two different Δt and SST steady state solution with reference LES (Fröhlich et al., [8]).

It is this robust behaviour with respect to space and time resolution which makes the SAS model an attractive concept for engineering simulations. In many technical flows, the quality of the grid and a proper LES time step cannot be maintained in the entire unsteady flow domain. The SAS model will however always have a fall-back URANS or RANS solution if the resolution is not sufficient for resolving the turbulent scales. In contrast, LES and DES models can return undefined model formulations and potential numerical instabilities under those conditions, as the eddy viscosity can be unphysically reduced.

The limitation of SAS is that it will not switch into scale-resolving mode if the flow is not sufficiently unstable. In this case, unsteady behaviour cannot be enforced at current point. If this is the case, the next step is switching to DES, which allows a reduction of the RANS eddy viscosity by reducing the grid spacing. This in turn is often sufficient for rendering the simulation unsteady. As stressed before however, the grid and time step will then have to be crafted carefully to avoid stress depletion and/or grey zones (meaning undefined model behaviour somewhere between RANS and LES).

If the flow instability is still not sufficient for producing the required unsteady structures, an interface or forcing terms need to be activated between the RANS and LES zones. Examples of such cases have been reported by Davidson [5]. The cases studied there are all dominated by the turbulence coming from the upstream boundary layers and are therefore not suitable for unsteady SAS or DES model simulations without an explicit conversion of energy to the resolved part (e.g. forcing). An example of such forcing with the SAS model can be found in Menter et al. [23].

In that respect all the modelling concepts from SAS-DES-LES will find their proper range of applications. From an engineering standpoint, the question is not “which model is better?”, but “which model is better for a given class of applications?” For strongly unstable flows the pendulum will likely swing towards the SAS model, for less unstable flows towards DES or even further to more advanced embedded LES models.

The flow around a triangular cylinder (Sjunnesson et al., [34]) constitutes a perfect example of a case suitable for SAS model simulations. Figure 12 shows the 2-D section of the grid used. It is extended in the third direction to cover 5 times the edge of the triangle. The overall grid size is $1.8 \cdot 10^6$ hexahedral cells. The Reynolds number is 45,500 with an inlet velocity of 17.3 m/s. Periodic boundary conditions are applied in spanwise direction. The simulations were run with ANSYS-Fluent using the BCD (bounded central difference) advection scheme

and a time step of $\Delta t=10^{-5}$ s. Since the separation occurs at the corner of the geometry, no attempt of resolving the boundary layers was made.

This testcase was computed with the SST-SAS and the SST-DES model. Figure 13 shows the turbulent structures for both models using $Q=10^6$ $1/s^2$. There is clearly very little difference between the two pictures indicating that such unstable flows do not necessarily require the application of hybrid models like DES but can also be captured by advanced URANS models like SAS.

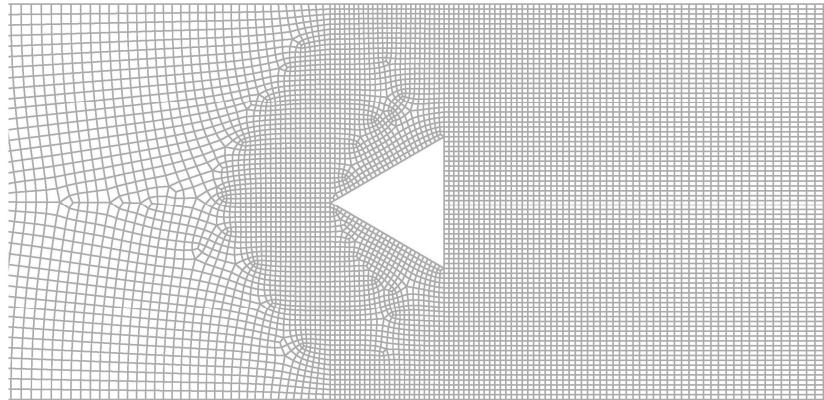


Figure 12: Numerical grid for flow around triangular cylinder.

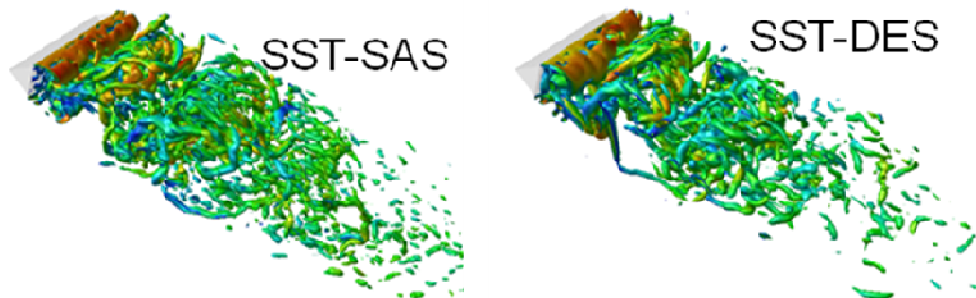


Figure 13: Flow structures for flow around triangular cylinder. Left: SST-SAS model, right: SST-DES model.

Figure 14 shows the mean axial velocity along the centreline behind the cylinder in comparison with the experimental data. The agreement of both models with the data is very close. The same is true for the comparison of the velocity profiles at

three different stations shown in Figure 15. The agreement between the SST-SAS model, the SST-DES model and the experiment is basically within the experimental uncertainties.

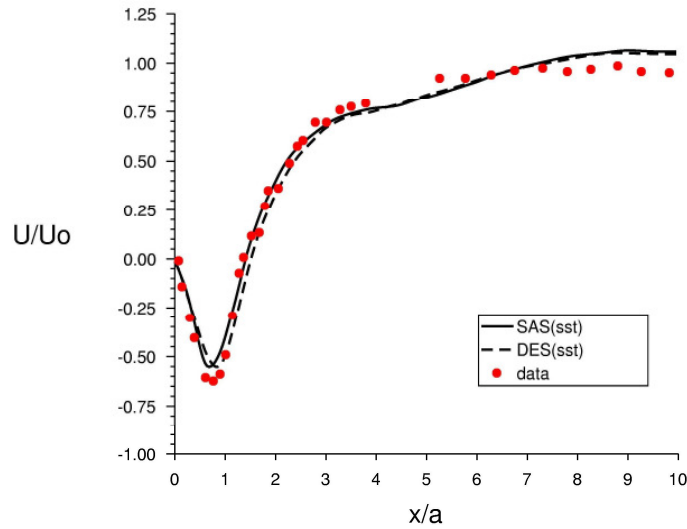


Figure 14: Mean axial flow velocity along centreline behind the triangular cylinder. Comparison of SST-SAS, SST-DES models and experiment.

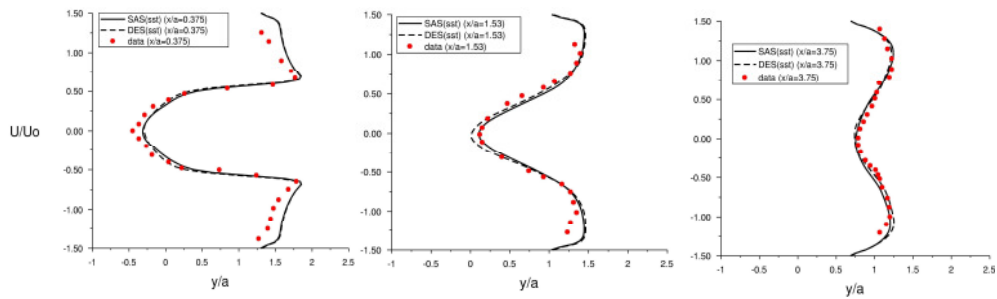


Figure 15: Velocity profiles for three different stations downstream of the triangular cylinder ($x/a=0.375$, $x/a=1.53$, $x/a=3.75$). Comparison of SST-SAS, SST-DES models and experiment.

In engineering flows there are frequently flow regions of the nature represented by the above testcase – e.g. large separation zones past bluff bodies. These areas are typically embedded within larger stable flow zones and are not predicted well by steady RANS methods. With SAS models, these areas are automatically “detected” and resolved down to the available grid and time step resolution limit.

If resolution is low, the model remains in RANS (or URANS) mode, making SAS a save pathway into scale-resolving engineering flow simulations.

In the companion article (Egorov et al., [7]), numerous more complex and industrially relevant testcases will be shown to demonstrate the SAS models potential for the simulation of engineering flows.

Summary

A new scale equation for turbulence modelling has been proposed. It is based on the usage of the exact length scale equation as derived by Rotta. It was argued that Rotta's rationale for avoiding the second derivative of the velocity field in favour of the third derivative is not consistent with the inhomogeneous nature of this term. The proposed model therefore features the second derivative in the source terms of the length scale equation. It was shown that the inclusion of this term is sensible, both from a theoretical as well as from a physical standpoint.

The central aspect of the article focused on the unsteady characteristics of SAS models. It was shown that the models exhibit both steady solutions and scale-resolving characteristics depending on the flow situation. The main difference to standard RANS models was illustrated for the Decaying Isotropic Turbulence in a box. While standard models damp out the resolved scales quickly, the SAS modelling approach allows the formation of a turbulent spectrum. Contrary to expectations, SAS models do not provide sufficient damping at the high wave number end. A limiter was proposed which ensures a proper LES limit of the formulation.

Two other examples have been shown to illustrate the behaviour and the potential of this method for unsteady flow predictions. The SAS approach can also serve as a basis for acoustics simulations, as it is able to generate the source terms for the acoustics simulation provided that the flow is sufficiently unstable.

The limitation of the current SAS methodology is that unsteadiness cannot be enforced for flows for which the model produces a steady solution. The next step

in the development of the SAS methodology is the inclusion of forcing terms to allow a transfer of modelled to resolved turbulence, thereby enforcing unsteadiness (Menter et al, [23]). It is also believed that SAS models offer interesting alternative for hybrid RANS-LES methods, as they are more compatible with LES formulations than standard RANS models.

Acknowledgement

The current work was partially supported by the EU within the research projects DESIDER (Detached Eddy Simulation for Industrial Aerodynamics) under contract No. AST3-CT-200-502842 (<http://cfd.mace.manchester.ac.uk/desider/>)

References

1. Baldwin, B. S., and Barth, T. J., : A One-Equation Turbulence Transport Model for Aerodynamic Flows," AIAA Paper 92-0439, (1992).
2. Coles, D. and Wadcock, A.J.,(1979): Flying Hot-Wire Study of Flow Past an NACA 4412 Airfoil at Maximum Lift, AIAA J., vol. 17, no. 4, pp. 312-329, (1979).
3. Comte-Bellot, G. and Corrsin, S.: Simple Eulerian time correlation of full- and narrow-band velocity signals in grid-generated, 'isotropic' turbulence, J. Fluid Mech., Vol. 48, Part 2, pp. 273-337, (1971).
4. Craft T J, Launder B E. and Suga K, Development and application of a cubic eddy-viscosity model of turbulence, Int. J. of Heat and Fluid Flow, 17(2):108–115, (1996).
5. Davidson, L.: Evaluation of the SST-SAS Model: Channel Flow, Asymmetric Diffuser and Axi-Symmetric Hill, Proceedings European Conference on Comp. Fluid Dyn. ECCOMAS CFD (2006).
6. Egorov, Y, and Menter F.R.,: Development and Application of SST-SAS Model in the DESIDER Project, in Advances in Hybrid RANS-LES Modelling, Notes on Num. Fluid Mech. And Multidisciplinary Design, Volume 97, Springer, (2008).
7. Egorov, Y, Menter, F.R. and Cokljat D.; Scale-Adaptive Simulation Method for Unsteady Flow Predictions. Part 2: Application to Aerodynamic Flows, companion paper, same journal, (2009).
8. Fröhlich J., Mellen C.P., Rodi W., Temmerman L., Leschziner M.,: Highly resolved large-eddy simulation of separated flow in a channel with streamwise periodic constrictions, J. of Fluid Mech., vol. 526, pp. 19-66, (2005).
9. Gatski, T.B., and Speziale C.G.,: On explicit algebraic stress models for complex turbulent flows, J. Fluid Mech., 254, 59-78, (1993).

10. Kim, S.E.: Large Eddy Simulation using Unstructured Meshes and Dynamic Subgrid-scale Turbulence Models. AIAA Paper no. 2004-2548, (2004).
11. Launder, B.E. and Spalding, D.B.: The Numerical Computation of Turbulent Flows, Comp. Meth. Appl. Mech. Eng, Vol. 3 pp.269-89, (1974).
12. Launder, B.E., Reece, G.J., W. Rodi,: Progress in the Development of a Reynolds-Stress Turbulence Closure, J. Fluid Mech. 68, 537, (1975).
13. Menter, F.R.: Two-equation eddy-viscosity turbulence models for engineering applications, AIAA Journal, Vol. 32, No. 8, pp. 1598-1605, (1994).
14. Menter, F. R.: Eddy viscosity transport equations and their relation to the k- ϵ model, NASA-TM-108854, (1994).
15. Menter F.R: Eddy viscosity transport equations and their relation to the k- ϵ model, Journal of Fluids Engineering, 119, pp. 876–884, (1997).
16. Menter, F. R, Kuntz, M., Bender R.: A scale-adaptive simulation model for turbulent flow predictions, AIAA Paper 2003-0767, (2003).
17. Menter F. R. and Egorov, Y.: Re-visiting the turbulent scale equation, Proc. IUTAM Symp. One Hundred Years of Boundary Layer Research, Göttingen, Springer (2004).
18. Menter F. R. and Egorov, Y.: A Scale-Adaptive Simulation Model using Two-Equation Models, AIAA Paper 2005-1095, Reno/NV, (2005).
19. Menter F. R. and Egorov, Y.: Turbulence Models based on the Length-Scale Equation, Fourth International Symposium on Turbulent Shear Flow Phenomena, Williamsburg, 2005 – Paper TSFP4-268, (2005).
20. Menter F. R. and Egorov, Y.: SAS Turbulence Modelling of Technical Flows, DLES 6 - 6th ERCOFTAC Workshop on Direct and Large Eddy Simulation September, Poitiers, (2005)
21. Menter F. R. and Egorov, Y., and Rusch D.: Steady and Unsteady Flow Modelling Using the $k - \sqrt{k}L$ Model, Proc. Turbulence, Heat and Mass Transfer 5, K. Hanjalic, Y. Nagano and S. Jakirlic (Editors), (2006).
22. Menter, F.R. and Egorov, Y.: Formulation of the Scale-Adaptive Simulation (SAS) Model during the DESIDER Project, In Notes on Num. Fluid Mech. and Multidisc. Design, Eds. W. Haase, M. Braza, A. Revell, Volume 103, Springer, (2009).
23. Menter F.R., Garbaruk A., Smirnov P.: Scale adaptive simulation with artificial forcing, Proc. 3rd Symposium on Hybrid RANS-LES Methods, (2009).
24. Moffatt, H. K. : Turbulence and Stochastic Processes: Kolmogorov's Ideas 50 Years, On. Edited by J. C. R. HUNT, O. M. PHILLIPS and D. WILLIAMS. Proceedings of the Royal Society, London, A, vol. 434, 1991, pp. 1–240, (1991).
25. Nicoud, F. and Ducros, F., Subgrid-scale stress modelling based on the square of the velocity gradient tensor. Flow, Turb. Combust. 62, 183-200, (1999).
26. Pope, S.B.: A more general effective-viscosity hypothesis, J. Fluid Mech., 72, pp. 331–340, (1975).
27. Rodi, W.: A new algebraic relation for calculating the Reynolds stresses, Z. Angew. Math. Mech, Vol. 56, pp 219-221, (1976).

28. Rodi, W.: Turbulence Modelling for Boundary Layer Calculations, Proc. IUTAM Symp. One Hundred Years of Boundary Layer Research, Göttingen, Springer (2004).
29. Rotta, J.C.: Über eine Methode zur Berechnung turbulenter Scherströmungen, Aerodynamische Versuchsanstalt Göttingen, Rep. 69 A14, (1968).
30. Rotta J. C.: Turbulente Strömungen. BG Teubner Stuttgart, (1972).
31. Spalart, P. R. and Allmaras, S. R.: A One-Equation Turbulence Model for Aerodynamic Flows, La Recherche Aérospatiale n 1, 5-21, (1994).
32. Spalart P. R.: Strategies for turbulence modelling and simulations, Int. J. Heat Fluid Flow, 21, pp. 2, (2000).
33. Spalart, P.R., Jou, W., Strelets, M., Allmaras, S.: Comments on the feasibility of LES for wings, and on a hybrid RANS/LES approach. In: Advances in DNS/LES, 1st AFOSR Int. Conf. on DNS/LES, (1997).
34. Sjunnesson, A., Henriksson, R. and Lofstrom C.: CARS measurements and Visualization of Reacting Flows in Bluff Body Stabilized Flame. AIAA Paper 92 – 3650, (1992).
35. Strelets, M.: Detached Eddy Simulation of massively separated flows. AIAA Paper 2001-879, (2001).
36. Wallin, S. and Johansson, A.V.: An explicit algebraic Reynolds stress model for incompressible and compressible turbulent flows, J. Fluid Mech., 403, pp. 89–132, (2000).
37. Wilcox, D. C.: Turbulence Modeling for CFD DCW Industries Inc., 2. Edition (1998).